NASA Technical Memorandum 100555

LATERAL AND LONGITUDINAL STABILITY AND CONTROL PARAMETERS FOR THE SPACE SHUTTLE DISCOVERY AS DETERMINED FROM FLIGHT TEST DATA

William T. Suit and
James R. Schiess

February 1988

National Aeronautics and
Space Administration

Langley Research Center
Hampton, Virginia 23665-5225

SUMMARY

The Discovery vehicle was found to have longitudinal and lateral aerodynamic characteristics similar to those of the Columbia and Challenger vehicles. The lateral aerodynamic characteristics of the Columbia and Challenger vehicles are reiterated and the results from the Discovery flight test are added to this data base. The longitudinal aerodynamics resulting from the analysis of flight data from all three vehicles are also shown. The values of the lateral and longitudinal parameters are compared with the preflight data book. The lateral parameters showed the same trends as the data book. With the exception of C_{ℓ_β} for Mach numbers greater than 15, $C_{n_{\delta r}}$ for Mach numbers greater than 2 and for Mach numbers less than 1.5, where the variation boundaries were not well defined, ninety percent of the extracted values of the lateral parameters fell within the predicted variations.

The longitudinal parameters showed more scatter, but scattered about the preflight predictions. With the exception of the Mach 1.5 to .5 region of the flight envelope, the preflight predictions seem a reasonable representation of the Shuttle aerodynamics. The models determined accounted for ninety percent of the actual flight time histories.

INTRODUCTION

During the design of the Space Shuttle, large quantities of wind-tunnel data were accumulated. This information was assembled into a data base which is assumed to describe the aerodynamic characteristics of the Shuttle vehicle over a large range of flight conditions. The resulting document will be referred to as the preflight data book (ref. 1).

Special maneuvers were performed during the development flights of the Shuttle for the purpose of determining the stability and control parameters at selected points on the descent trajectory. Even after the Shuttle became operational, a limited number of maneuvers were performed during the descent to the landing site. The responses to these maneuvers were analyzed and the stability and control parameters obtained were used to augment the preflight data base. The flight-derived aerodynamics were used to verify the preflight data book and to suggest areas of the preflight analysis that did not accurately predict the aerodynamic characteristics of the vehicle.

The results of these analyses for the lateral aerodynamic parameters for the Columbia and Challenger vehicles have been assembled and reports using the flight-determined parameters from the first eight Shuttle flights have been presented at a number of conferences (refs. 2-6). The main emphasis in the analysis of Shuttle flight data has been on the identification of the lateral aerodynamics of the vehicle because the preflight analyses indicated potential lateral instabilities in some flight regimes. The longitudinal aerodynamic parameters were determined from selected runs for the Columbia and Challenger Shuttle vehicles and these results will be presented.

This paper will supplement the existing flight-derived parameter data base by adding both longitudinal and lateral results using flight test data from the Space Shuttle Discovery. These results will be compared with the longitudinal and lateral results from Columbia and Challenger. The maneuvers performed using Discovery are similar to those used with Columbia and Challenger.

SYMBOLS

a_X, a_Y, a_Z	acceleration measured along X, Y, and Z body axes, respectively, g units
b	wing span, m (ft)
$\bar{c}$	wing mean geometric chord, m (ft)
C_ℓ	rolling-moment coefficient, $M_X/\bar{q}Sb$
$C_{\ell o}, C_{no}$	aerodynamic moments for trimmed flight
C_m	pitching-moment coefficient, $M_Y/\bar{q}S\bar{c}$
C_n	yawing-moment coefficient, $M_Z/\bar{q}Sb$
C_X	axial-force coefficient, $F_X/\bar{q}S$
C_{Yo}	aerodynamic force for trimmed flight
C_Y	lateral-force coefficient, $F_Y/\bar{q}S$
C_{Zo}	trim coefficient
C_Z	normal-force coefficient, $F_Z/\bar{q}S$
e	vector of measurement error
F	vector function representing equations of motion
F_X, F_Y, F_Z	force along X, Y, and Z body axes, respectively, N(lb)
g	acceleration due to gravity, 9.81 m/sec^2 (32.2 ft/sec^2)
G	vector function representing measurement equations
I_X, I_Y, I_Z	moment of inertia about X, Y, and Z body axis, respectively, kg-m^2 (slug-ft^2)
I_{XZ}	product of inertia, kg-m^2 (slug-ft^2)
J	cost function
k	number of data points
L	likelihood function
m	mass, kg (slugs)
M_X, M_Y, M_Z	rolling, pitching, and yawing moments, respectively, N-m (ft-lb)
p,q,r	rate of roll, pitch and yaw, rad/sec or deg/sec

$\bar{q}$	dynamic pressure, $\rho V^2/2$, Pa (psi)
R	measurement noise covariance matrix
S	wing area, m^2 (ft^2)
t	time, sec
u	velocity along X-body axis, m/sec (ft/sec)
U	input vector
v	velocity along Y-body axis, m/sec (ft/sec)
V	airspeed, m/sec (ft/sec)
w	velocity along Z-body axis, m/sec (ft/sec)
X	vector of states
Y	vector of outputs
α	angle of attack, rad
β	sideslip angle, rad
δa	aileron deflection, rad
δe	elevator deflection, rad or deg.
δr	rudder deflection, rad
δRCS	RCS control term, number of jets firing
Ω	vector of unknown parameters
θ	pitch angle, rad
ϕ	roll angle, rad
$\dot{\phi}_o$	bias on roll rate, rad/sec

Subscripts:

i	quantity at i^{th} time
M	measured quantity
p,q,r	rotary derivatives
α	static derivatives with respect to α
β	static derivatives with respect to β
$\delta a, \delta e, \delta r, \delta RCS$	control derivatives with respect to indicated quantity

t	trimmed value
X,Y,Z	longitudinal, lateral, and vertical body axes

Matrix exponents:

T	transpose of matrix
-1	inverse of matrix

Mathematical notation:

^	estimated quantity when over symbol
·	derivative with respect to time when over symbol
∇	gradient operator

Abbreviations:

ACIP	Aerodynamic Coefficient Identification Package
BET	Best Estimated Trajectory
IMU	Inertial Measurement Unit
LaRC	Langley Research Center
MMLE3	Modified Maximum Likelihood
PTI	Programmed Test Input
RCS	Reaction Control System
RGA,AA	Rate Gyro Assembly, Accelerometer Assembly
STS	Space Transportation System

TEST VEHICLE

The orbiter configuration is shown in figure 1 and key physical characteristics are given in Table 1. The thick, double delta wing is configured with full span elevons, comprised of two panels per side. Each elevon panel is independently actuated. All four panels are deflected symmetrically as an elevator for pitch control, and left and right elevons are deflected differentially as an aileron (δa) for roll control.

The body flap is used as the primary longitudinal trim device. The elevons are programmed in conjunction with the body flap to follow a set schedule to provide the desired aileron effectiveness.

The vertical tail consists of the fin and a split rudder. The rudder panels are deflected for yaw control and are separated to act as a speed brake to provide for subsonic energy modulation. The speed brake opens fully (87.2 degrees) just below Mach 10 and then follows a predetermined schedule until Mach 0.9 is reached. The rudder is not activated until Mach 5.

Stability augmentation is provided by the aft reaction control system (RCS) jets, with the forward jets reserved for on-orbit attitude control and for abort maneuvers. The aft yaw jets are active until Mach 1, while the pitch and roll jets are terminated at a pressure of 20 and 10 pounds per square foot, respectively. Additional details of the Shuttle vehicle and its systems are given in reference 1.

MANEUVERS

Specially designed maneuvers were performed to obtain data for use in extracting aerodynamic parameters. These maneuvers were performed to obtain data at specific points during the descent trajectory. The test points were chosen so that aerodynamic parameters could be determined along the descent trajectory to verify the aerodynamic model obtained from the wind tunnel tests. This verification procedure will add confidence to the assumed aerodynamics of the Shuttle where there is agreement and will point to areas of potential inaccuracy where there is no agreement.

The actual forms of the inputs to be performed were developed using a Shuttle simulation to generate responses for various inputs and then extracting parameters from these responses. The control inputs that gave the best definition of the parameters of interest were then used for the flight tests. In spite of the care taken to design effective inputs, because the automatic control system was active, the controls were coupled and the resulting responses were reduced in magnitude and correlated with each other and the control inputs. This led to identifiability and correlation of parameter problems during the extraction process. Additional details on the maneuver design are given in reference 7.

INSTRUMENTATION AND DATA PROCESSING

As a development vehicle, the Shuttle is fully instrumented and has a number of redundant systems for measuring various vehicle states and controls. The instrument packages will be mentioned specifically. First is the Aerodynamic Coefficient Identification Package (ACIP), an instrumentation package specifically designed to measure rates, accelerations, and control surface positions required for parameter identification. The ACIP data were recorded at 172 samples per second. Second is

the instrumentation for the flight guidance and control system, the Rate Gyro Assembly and Accelerometer Assembly (RGA,AA), which is a source for acceleration and rate measurements. The RGA,AA data were recorded at 25 samples per second but are very noisy. The third source of flight measurements is the navigation instrumentation, the Inertial Measurement Unit (IMU). The IMU measurements are high fidelity but are recorded at only one sample per second which limits their usefulness.

The ACIP data were the primary source for the linear and angular accelerations, angular rates and control surface deflections. The RCS chamber pressures were used to determine the jet thrust, and these measurements came from the vehicle operational instrumentation.

The data considered most reliable were used to generate a best estimated trajectory (BET) for the Shuttle vehicle. The data written to tapes for the parameter extraction consisted of only those maneuvers considered appropriate for extraction. The linear and angular rates and control surface deflections came from the ACIP instrumentation. The BET angular rates and linear accelerations at the start of a maneuver were taken as initial conditions, and the rates and accelerations were integrated over time to obtain angular positions and vehicle velocities. The velocities were then corrected for the effect of winds, and the resulting components were used to calculate the vehicle total velocity, angle of attack, and angle-of-sideslip. This combined data set is recorded at 25 samples per second and comprises the data contained on the tape to be processed by the parameter extraction software. Additional details on the instrumentation and data processing can be found in references 8, 9, and 10.

EQUATIONS OF MOTION

The lateral-direction equations of motion used in this study are based on perturbations about trimmed flight conditions and are written relative to the body axes shown in figure 1. The equations are

$$\dot{v} = -ru + pw + g \cos\theta \sin\phi + \frac{\bar{q}S}{m} C_Y \tag{1}$$

$$\dot{p} = \frac{I_{XZ}}{I_X} \dot{r} + \frac{I_Y - I_Z}{I_X} qr + \frac{I_{XZ}}{I_X} pq + \frac{\bar{q}Sb}{I_X} C_\ell \tag{2}$$

$$\dot{r} = \frac{I_{XZ}}{I_Z} \dot{p} + \frac{I_X - I_Y}{I_Z} pq - \frac{I_{XZ}}{I_Z} qr + \frac{\bar{q}Sb}{I_Z} C_n \tag{3}$$

$$\dot{\phi} = p + r \cos\phi \tan\theta + \sin\phi \tan\theta + \dot{\phi}_o$$

$$a_Y = \frac{1}{g} (\dot{v} + ru - pw - g \cos\theta \sin\phi) \tag{4}$$

where

$$C_Y = C_{Y_o} + C_{Y_\beta}\beta + C_{Y_p}\frac{pb}{2V} + C_{Y_r}\frac{rb}{2V} + C_{Y_{\delta r}}(\delta r - \delta r_t)$$

$$+ C_{Y_{\delta a}}(\delta a - \delta a_t) + C_{Y_{\delta RCS}}\delta RCS \tag{5}$$

$$C_\ell = C_{\ell_o} + C_{\ell_\beta}\beta + C_{\ell_p}\frac{pb}{2V} + C_{\ell_r}\frac{rb}{2V} + C_{\ell_{\dot\beta}}\frac{\dot\beta b}{2V} + C_{\ell_{\delta r}}(\delta r - \delta r_t)$$

$$+ C_{Y_{\delta a}}(\delta a - \delta a_t) + C_{Y_{\delta RCS}}\delta RCS \tag{6}$$

$$C_n = C_{n_o} + C_{n_\beta}\beta + C_{n_p}\frac{pb}{2V} + C_{n_r}\frac{rb}{2V} + C_{n_{\dot\beta}}\frac{\dot\beta b}{2V} + C_{n_{\delta r}}(\delta r - \delta r_t)$$

$$+ C_{n_{\delta a}}(\delta a - \delta a_t) + C_{n_{\delta RCS}}\delta RCS \tag{7}$$

The results of this study are based on maneuvers performed at velocities of Mach 1 and higher. For this reason the terms containing velocity are sufficiently small that the equations of motion are considered essentially insensitive to the rotary derivatives and to $C_{\ell_{\dot\beta}}$ and $C_{n_{\dot\beta}}$; therefore, these derivatives are fixed at zero throughout this study.

The equations used to describe the longitudinal motions were

$$\dot u = -qw + rv - g\sin\theta + \frac{\bar q S}{m}C_X \tag{8}$$

$$\dot w = -pv + qu + g\cos\theta\cos\phi + \frac{\bar q S}{m}C_Z \tag{9}$$

$$\dot q = pr\,\frac{I_Z - I_X}{I_Y} + \frac{I_{XZ}}{I_Y}(r^2 - p^2) + \frac{\bar q S\bar c}{I_Y}C_m \tag{10}$$

$$\dot\theta = q\cos\phi - r\sin\phi \tag{11}$$

$$a_X = \frac{1}{g}(\dot u + qw - rv + g\sin\theta) \tag{12}$$

$$a_Z = \frac{1}{g}\left(\dot{w} + pv - qu - g\cos\theta\cos\phi\right) \tag{13}$$

$$V = \sqrt{u^2 + v^2 + w^2} \tag{14}$$

$$\alpha = \tan^{-1}\frac{w}{u} \tag{15}$$

$$\beta = \sin^{-1}\frac{v}{V} \tag{16}$$

$$C_X = C_{X,o} + C_{X_\alpha}(\alpha - \alpha_t) \tag{17}$$

$$C_Z = C_{Z,o} + C_{Z_\alpha}(\alpha - \alpha_t) + C_{Z_q}\frac{q\bar{c}}{2V} + C_{Z_{\delta e}}\left(\delta_e - \delta_{e_t}\right) \tag{18}$$

$$C_m = C_{m,o} + C_{m_\alpha}(\alpha - \alpha_t) + C_{m_q}\frac{q\bar{c}}{2V} + C_{m_{\delta e}}\left(\delta_e - \delta_{e_t}\right) \tag{19}$$

MAXIMUM LIKELIHOOD ESTIMATION

Stability and control derivatives were extracted using the maximum likelihood estimator. Among other statistical properties, the maximum likelihood estimator is asymptotically efficient and asymptotically unbiased. This estimator consists of maximizing the likelihood function of the measurement errors, which is the product of the probability density functions evaluated at each measurement time. This approach requires that the form of the measurement error distribution is known; it is normally assumed this distribution is Gaussian.

It is assumed the actual system can be modeled as

$$\dot{X}(t) = F(X,U,\Theta,t) \tag{20}$$

$$Y(t_i) = G(X,U,\Theta,t_i) + e_i, \qquad i = 1,2,\ldots,k \tag{21}$$

where equation (20) is a vector representation of equations (1) to (4) or equations (8) to (13) and equation (21) is a vector representation of the measurements. In these equations, X is the state vector, U the vector of controls, Θ the vector of stability and control derivatives, t is time, and e_i the vector of measurement noise for the measurements at time t_i.

If it is assumed that the measurement noise is Gaussian, then the likelihood function (ref. 11) is

$$L(Y,\Theta) = \left[(2\pi)^4 R\right]^{-k/2} \exp\left\{-\frac{1}{2}\sum_{i=1}^{k}\left[Y_M(t_i) - Y(t_i)\right]^T R^{-1}\left[Y_M(t_i) - Y(t_i)\right]\right\} \tag{22}$$

where the subscript M denotes actual measurements and R is the measurement covariance matrix. Taking the natural logarithm of equation (22) and multiplying by -1 yields the cost function

$$J(\Theta) = -\log L(Y,\Theta) = \frac{1}{2}\sum_{i=1}^{N}\left[Y_M(t_i) - Y(t_i)\right]^T R^{-1}\left[Y_M(t_i) - Y(t_i)\right]$$

$$+ \frac{N}{2}\log R + 2N \log 2\pi \tag{23}$$

Maximization of equation (22) with respect to Θ is equivalent to minimization of equation (23) with respect to Θ. The last term on the right is constant relative to Θ and can be neglected; if R is known, the second term can also be neglected for the same reason. Minimization of the remaining term results in solving $\nabla J_{\Theta=\hat{\Theta}} = 0$ which gives the estimates

$$\hat{\Theta}_{j+1} = \hat{\Theta}_j - \left[\nabla^2 J(\hat{\Theta}_j)\right]^{-1} \nabla J(\hat{\Theta}_j), \quad j = 0,1,2,\ldots \tag{24}$$

Since a sequence of estimates, $\hat{\Theta}_j$, are obtained iteratively, the process must begin with initial parameter estimates, $\hat{\Theta}_o$.

If R is unknown in equation (23), direct minimization of $J(\Theta)$ with respect to Θ and R is complicated by the fact that R is an implicit function of Θ. A simpler approach is to minimize with respect to Θ and R independently. Minimization of equation (23) with respect to R yields

$$\hat{R} = \frac{1}{N}\sum_{i=1}^{N}\left[Y_M(t_i) - Y(t_i)\right]\left[Y_M(t_i) - Y(t_i)\right]^T \tag{25}$$

The procedure used here is, first, assuming $\hat{R}$ is diagonal with initial estimates for the diagonal elements, iterate equation (24) several times. Then, on each succeeding iteration, first estimate $\hat{R}$ using the most recent value of $\hat{\Theta}$ in equations (21) and (25), and then apply equation (24) once using $\hat{R}$ in $J(\Theta)$. This two step process is repeated each iteration to convergence.

The data from flight tests for the three Shuttle vehicles were analyzed using two Maximum Likelihood parameter extraction computer programs (refs. 11 and 12). The two programs were used independently by two investigators, and when the same data were processed, similar parameter values were determined. The parameter values resulting from processing the different Shuttle flights were plotted versus Mach number, and these plots form the basis for the discussion.

ANALYSIS AND RESULTS

In this section the results obtained in this study are discussed. These results are based on extracting the stability and control derivatives from 16 PTI maneuvers on the three flights. The time span for the measurements obtained during the maneuvers ranged from 4 to 15 seconds with the measurements sampled 25 times a second.

The estimation approach taken here is based on information contained in measured accelerations and rates, various trajectory parameters and the measured atmosphere. The method of analyzing atmospheric measurements which accounts for spatial, diurnal, and semidiurnal corrections is described by Price (ref. 13). This atmospheric information is combined with onboard measurements of accelerations and rates in order to construct the trajectory (ref. 14) which is used for estimating the stability and control derivatives.

In the results presented, lateral moment derivatives are relative to the flight center of gravity and were estimated with rotary derivatives fixed at zero and $C_{Y_{\delta a}}$ fixed at the data book value of 0.00042 per degree. The longitudinal derivatives $C_{Z_{\delta e}}$ and C_{mq} were fixed at data book values. All mass properties and center of gravity information were supplied by NASA Johnson Space Center and are shown in Table I. The lateral time histories fit during the estimation process were: β, p, r, ϕ, and a_Y and the longitudinal time histories fit were V, α, q, and a_Z. For the lateral runs using the estimation method of reference 11 the weighting matrix (inverse of the measurement noise covariance matrix, $\hat{R}$) was initially set to a diagonal matrix with the values 796.3, 234.8, 4324, 237.5, and 21820. These values correspond, respectively, to the measured variables β, p, r, ϕ, and a_y. Estimation of $\hat{R}$ using equation (25) began on iteration 4 for each maneuver; from 8 to 20 iterations were required for convergence. When the estimation method of reference 12 was used, the weighting matrix was calculated based on the fit to the data from the initial guess at the parameter values used in the mathematical model to be estimated.

The extracted stability and control derivatives will be presented in figures as functions of Mach number. Both flight-extracted and predicted values along with variations associated with the predicted values will be shown. For example, figure 2 shows rolling moment due to sideslip angle as a function of Mach number with the predicted values (P) and variations (V) indicated by solid lines and the extracted values by various symbols. The predicted values are based on data book values, which are the result of numerous preflight tests of Shuttle aerodynamics (ref. 1). The actual procedure for developing the predicted derivative time histories is given in reference 9. The variations reflect uncertainties in the data book values; they are based on differences between flight and predicted results for previously researched aircraft and extrapolated to the Shuttle configuration. The uncertainties were not developed for the longitudinal motion derivatives.

The discussion of the results will be split into two parts: one for presentation of the lateral maneuver results and one for the presentation of the longitudinal maneuver results.

Lateral Maneuvers

The results obtained from analysis of the lateral maneuvers will be examined in three parts: the sideslip parameters, the aileron effectiveness parameters, and the rudder effectiveness parameters.

Side-Slip Parameters. C_{y_β} - The side force due to sideslip parameter is shown plotted versus Mach number in figure 2. This parameter tended to be difficult to identify, and the Cramer-Rao bounds were generally greater than 10 percent of the extracted value for the parameter. If there is a trend, the Challenger tends to show less C_{y_β}. At the lower Mach number C_{y_β} becomes more negative, but how much is not clear.

The trends for the Discovery vehicle seem to follow the preflight predictions well except for the scatter at the lowest Mach numbers. The results show no significant differences between the Discovery vehicle and the Columbia and Challenger vehicles (fig. 2). For the C_{y_β} parameter, the preflight prediction offers a reasonable description of this derivative.

C_{ℓ_β} - The rolling moment due to sideslip parameter was well determined, and the Cramer-Rao bounds were generally less than 2 percent of the extracted parameter value. The values of C_{ℓ_β} were less negative than predicted at the highest Mach numbers (fig. 2). The values determined from the Discovery flight data consistently followed this trend established by the other vehicles. In fact, the Discovery results were generally more consistent run-to-run than those of the other vehicles for most of the Mach range. Below Mach 5, there is considerable scatter in the C_{ℓ_β} values extracted for all the vehicles (fig. 2). In this Mach range, the general trend agrees with the preflight predictions and indicates a C_{ℓ_β} value near zero for Mach number less than 1. The preflight predictions are a reasonable representation of C_{ℓ_β} for the mid to low Mach numbers (fig. 2).

C_{n_β} - The yawing moment with sideslip angle parameter is shown plotted versus Mach number in figure 2. The flight determined C_{n_β} generally agrees with the preflight predictions for all vehicles. Only in the Mach 5 to Mach 10 range do the values tend to be more negative than predicted. The trends below Mach 5 seem to be more clearly defined for all vehicles than for most of the other parameters extracted (fig. 2). Again, the C_{n_β} values extracted from the Discovery flight data agree very well with the values determined from the flight data of the other two Shuttle vehicles.

Aileron Control Effectiveness. $C_{\ell_{\delta a}}$ - The rolling moment due to aileron versus Mach number is shown in figure 3a. The values extracted from flight data for all three vehicles showed the same trends as the preflight predictions. While the Cramer-Rao bounds for $C_{\ell_{\delta a}}$ were, in general, less than 2 percent of the extracted values, the scatter in the extracted values implies that the parameter may not be as well determined as C_{ℓ_β} and C_{n_β} (fig. 2). The Discovery vehicle aileron showed

less effectiveness than the other vehicles at high Mach numbers, but the limited data make conclusions difficult. As a general conclusion, for all Mach numbers, the preflight estimates seem to be a good representation of $C_{\ell_{\delta a}}$.

$C_{n_{\delta a}}$ - The yawing moment due to aileron parameter plotted versus Mach number is shown in figure 3b. The parameter was not especially well determined at the high Mach numbers, and the Cramer-Rao bounds are on the order of 10 percent of the extracted parameter value. In the Mach 18 to Mach 5 range, the determination was better, but the Cramer-Rao bounds were still high. Below Mach 5 $C_{n_{\delta a}}$ showed the same scatter that has been seen from most of the parameters. The values of $C_{n_{\delta a}}$ for the Discovery vehicle generally followed the same trends as those seen for the Columbia and Challenger vehicles; however, they seem to indicate slightly less aileron effect at the higher Mach numbers (fig. 3b). The values determined from flight data for all three vehicles followed the same trends as the preflight predictions. Hence, these predictions are a reasonable representation of the value of $C_{n_{\delta a}}$.

Rudder Control Effectiveness. $C_{\ell_{\delta r}}$ - The rolling moment due to rudder parameter plotted versus Mach numbers is shown in figure 4a. The parameter was well determined and the values extracted from flight data for each of the Shuttle vehicles showed trends similar to those of the preflight predictions. The $C_{\ell_{\delta r}}$ values determined using the Discovery flight data agreed well with the preflight predictions, even at the lower Mach numbers. Again, the parameters determined using flight test data are similar in value and trend to the preflight predictions indicating that the latter are reasonable for the $C_{\ell_{\delta r}}$ parameter.

$C_{n_{\delta r}}$ - The yawing moment due to rudder parameter plotted versus Mach number is shown in figure 4b. The parameter was well determined and did not show much scatter. The values determined using the Columbia and Challenger vehicles showed similar trends and values for $C_{n_{\delta r}}$. The values determined using the Discovery flight data agree well with those obtained using flight data from the other vehicles. However, for all vehicles $C_{n_{\delta r}}$ was consistently less effective than predicted above Mach 2.

In summary, the parameter values determined using data from the three vehicles agree very well. In most cases, the parameters, with Cramer-Rao bounds approximately 2 percent of the extracted value, agree well with the preflight predictions. As a further check, several places were found on the Discovery flight tape where there were aileron trim settings prior to maneuvers. For each aileron trim there was a trim sideslip angle and the ratio gave an indication of the C_{ℓ_β} to $C_{\ell_{\delta a}}$ ratio that might be expected from the maneuver. Since there were trim points at different Mach numbers, any variation in this ratio with Mach numbers should be indicated. The trim ratios, estimated C_{ℓ_β} to $C_{\ell_{\delta a}}$ ratios and the predicted C_{ℓ_β} to $C_{\ell_{\delta a}}$ ratios, are all given in Table II for several Mach numbers where the trim was well enough established to make the calculations. The data in the table show that the parameter ratios calculated from trim were in fair agreement with ratios determined using the extracted parameters, and both showed reasonable agreement with the preflight prediction ratios. The trends with Mach number were also predicted by the trim settings, indicating that the trends determined from the flight test for C_{ℓ_β} and $C_{\ell_{\delta a}}$ seem reasonable.

Longitudinal Maneuvers

Attempts to determine longitudinal aerodynamic parameters from flight data for the Shuttle vehicle have been only partially successful. Several factors contribute to this limited success. First, the perturbations that are allowed by safety considerations are so small that the vehicle cannot be disturbed sufficiently to have responses that are large enough for good parameter identification. Secondly, only the control surfaces are available to perturb the vehicle and these move so slowly that true step inputs cannot be used to disturb the vehicle. Responses to the slower inputs can lead to correlation problems during parameter extraction. Hence, a limited discussion of selected longitudinal parameters will be presented.

Because of identifiability and correlation problems, the longitudinal parameters will first be discussed as a group and then individual parameter characteristics will be discussed. The discussion will center on three longitudinal parameters: C_{Z_α}, the change in force along the "Z" body axis with angle-of-attack change; C_{m_α}, the pitching moment due to angle-of-attack change; and $C_{m_{\delta e}}$, the pitching moment due to elevon change. The motion of the Shuttle about some trim conditions resulting from a control input can be described using a set of equations containing C_{Z_0} (trim coefficient) and the three parameters under discussion. This reduced mathematical model will describe about 90 percent of the motion about the trim condition. Since the parameters C_{Z_α}, C_{m_α}, and $C_{m_{\delta e}}$ describe the majority of the vehicle motion, they can be identified with the greatest confidence, and only these parameters will be discussed in the paper. The three parameters are plotted versus Mach number and are shown as figure 5.

The $C_{m_{\delta e}}$ parameter was best defined with a Cramer-Rao bound less than 3 percent of the extracted parameter value. C_{Z_α} had Cramer-Rao bounds that were about 5 percent of the extracted value while C_{m_α} had bounds that were about 10 percent of the extracted value. $C_{m_{\delta e}}$ and C_{m_α} were correlated in almost all cases. In spite of the correlation and poor identifiability problems previously mentioned, C_{Z_α}, $C_{m_{\delta e}}$, and C_{m_α} generally showed trends similar to those of the preflight data book (fig. 5b and 5c).

C_{Z_α} - The parameter values determined showed that above Mach 15, C_{Z_α} was generally more negative than predicted (solid curve) when the Maximum Likelihood estimator was used (fig. 5a). In many cases below Mach 15 the values obtained using the Columbia flight data tended to be less negative than predicted while the values obtained using the Challenger data tended to be more negative than predicted. The trends seen using Columbia data were also evident in the results of reference 15. Values of C_{Z_α} calculated from steady-state relations showed trends close to those of the preflight predictions (fig. 5a). Most of these calculations were made using data from Columbia flights.

The values for C_{Z_α} obtained using the data from the first Discovery flight are similar to those for the Challenger vehicle. However, when the flight data from the second Discovery flight were used to determine C_{Z_α} above Mach 5, the values obtained were consistently less negative than the values obtained using the data from the first Discovery flight and from the Challenger flights (fig. 5a). An examination of the different sets of data showed that pulse-type commands were used to excite the vehicle for longitudinal parameter extraction during the Challenger flights and also

for the first Discovery flight. During the second Discovery flight doublet commands were used above Mach 5 to excite the vehicle. The actual elevon surface motion was not a true doublet because the automatic control system modified the input. A sample time history of the elevon inputs for the first and second Discovery flights is shown in figure 6. The parameter values extracted for each input are given in Table II. The C_{Z_α} value is clearly significantly different. In most cases the Cramer-Rao bounds were about 5 percent of the extracted parameter value implying some confidence in the values extracted.

When C_{Z_α} was fixed at the preflight predictions, $C_{m_{\delta e}}$ were unchanged or were close to the preflight values in a majority of the cases examined (fig. 5a). This new set of parameters still described about 90 percent of the perturbation from trim motion of the Shuttle. This implies that the restricted inputs could not excite the vehicle enough to identify all of the parameters in the assumed mathematical model, and that although C_{Z_α} seemed reasonably well identified, a change of over 50 percent in the parameter value did not have a serious effect on the fit to the data or the values of $C_{m_{\delta e}}$ and C_{m_α}. By fixing C_{Z_α} for selected runs throughout the Mach range, a model closer to the preflight predictions that still fits the flight data could be obtained. Below Mach 5, however, some questions still remain as to the best model to represent the Shuttle longitudinal aerodynamics and this will be addressed in the section discussing C_{m_α} and $C_{m_{\delta e}}$.

C_{m_α} and $C_{m_{\delta e}}$ - Since these parameters are correlated for most of the Shuttle runs examined, they will be discussed together. At the higher Mach numbers there was considerable scatter in the extracted values for C_{m_α}, but the trends generally followed those of the preflight predictions (fig. 5b). Below Mach 5, the values extracted for $C_{m_{\delta e}}$ tended to show less elevon effectiveness than predicted. For the Columbia vehicle this trend was also shown in reference 15. However, in the Mach greater than 5 range, when C_{Z_α} was fixed at the preflight predictions, $C_{m_{\delta e}}$ generally changed very little. While C_{m_α} variations were less that 10% for most cases there were some significant variations seen. This was not unexpected because C_{m_α} was not well identified. Since $C_{m_{\delta e}}$ is considered better defined than the other two parameters, the fit to the data did not suffer significantly.

For Mach less than 5, the trends of the extracted values of $C_{m_{\delta e}}$ and C_{m_α} followed the trends of the preflight predictions down to Mach numbers less than 2 (fig. 5). Below Mach 2 the preflight predictions show large variations in C_{m_α} and $C_{m_{\delta e}}$ (fig. 5). The magnitude of the C_{m_α} values generally followed the trends of the preflight estimates. However, the extracted values of $C_{m_{\delta e}}$ were generally 30 to 50 percent less than the predicted values. In this Mach range fixing C_{Z_α} did not significantly affect $C_{m_{\delta e}}$ in most cases, but some significant changes were seen in C_{m_α} (fig. 5b). The most serious difference between the preflight predictions of the longitudinal parameters and the flight determined parameters is the reduced elevon effectiveness as indicated by $C_{m_{\delta e}}$ around Mach 1. This is illustrated by considering the situation where both C_{Z_α} and $C_{m_{\delta e}}$ are set to the preflight predictions, then the values of C_{m_α} extracted were as much as 100 percent different from the preflight predictions, and in many cases, became positive. The fit also degraded for these cases. Although there are only five runs near Mach 1 where the

predicted $C_{m_{\delta e}}$ has the greatest magnitude, the preflight predictions imply more control effectiveness than was found using the flight test results.

Above Mach 5 the Discovery vehicle results show the same trends for C_{Z_α}, C_{m_α}, and $C_{m_{\delta e}}$ as the Challenger vehicle when the same control inputs were used to excite the vehicle. C_{Z_α} was consistently more negative than the preflight predictions. However, when a different input form was used, the values were considerably less negative than predicted. For the Columbia and Discovery maneuvers where C_{Z_α} was less negative than predicted, C_{m_α} and $C_{m_{\delta e}}$ still generally showed the same trends as seen with the Challenger and first Discovery flights.

In all cases using Discovery flight data taken above Mach 5, fixing C_{Z_α} at the preflight values resulted in a mathematical model that described the motion of the vehicle and that showed trends similar to those of the preflight predictions (fig. 5).

For $C_{m_{\delta e}}$ and C_{m_α} in the Mach number less than 5 range, the values estimated using Discovery data were close to the preflight predictions except around Mach 1, and fixing C_{Z_α} did not change these values significantly. As previously discussed, the values of $C_{m_{\delta e}}$ extracted from flight data in the Mach 1.5 to 0.6 range, were significantly different from the preflight predictions. However, for the rest of the Mach range, the preflight predictions should be considered a reasonable representation of the aerodynamics, not only of the Discovery vehicle, but for the Columbia and Challenger vehicles also.

CONCLUSIONS

The Discovery, Challenger, and Columbia all exhibited similar lateral and longitudinal aerodynamic characteristics. The preflight predictions are a reasonable representation of the Shuttle aerodynamics for all vehicles except for three cases. The first is for C_{ℓ_β} in the Mach number greater than 15 range where the flight-determined parameter value is smaller than predicted. The second exception is that $C_{n_{\delta r}}$ for Mach numbers greater than 2 was determined to indicate less rudder effectiveness than predicted. Thirdly, $C_{m_{\delta e}}$ in the Mach 1.5 to 0.6 range indicated approximately thirty percent less elevon effectiveness than predicted.

REFERENCES

1. Aerodynamic Design Data Book--Volume I: Orbiter Vehicle. NASA CR 160386, 1978.

2. Compton, Harold R.; Scallion, William I.; Schiess, James R.; and Suit, William T.: Shuttle Entry Performance and Stability and Control Derivatives Extraction from Flight Measurement Data. AIAA Paper No. 82-1317, 1982.

3. Compton, H. R.; Schiess, J. R.; Suit, W. T.; Scallion, W. I.; and Hudgins, J. W.: Evaluation of Shuttle Performance and Lateral Stability and Control over the Supersonic and Hypersonic Speed Range. NASA CP-2283, 1983.

4. Kirsten, P. W; and Richardson, D. F: Predicted and Flight Test Results of the Performance and Stability and Control of the Space Shuttle From Reentry to Landing. AGARD 61st Flight Mechanics Panels Meeting, Symposium of Ground/Flight Test Techniques and Correlation, Cesme, Turkey, October 11-15, 1982.

5. Cooke, Douglas R.: Minimum Testing of the Space Shuttle Orbiter for Stability and Control Derivatives. NASA CP-2283, Part 1, 1983, pp. 447-471.

6. Schiess, J. R.; Suit, W. T.; and Scallion, W. I.: Investigation of the Effect of Vehicle Angle of Attack and Trim Elevon Position on the Lateral-Directional Aerodynamic Parameters of the Shuttle Orbiter. AIAA Paper No. 87-2072, 1984.

7. Cooke, D. R.: Space Shuttle Stability and Control Test Plan. AIAA Paper No. 82-1315, 1982.

8. Findlay, J. T.; Kelly, G. M.; and Henry, M. W.: An Extended BET Format for LaRC Shuttle Experimenters: Definition and Development. NASA CR-165882, April 1982.

9. Findlay, J. T.; Kelly, G. M.; and McConnell, J. G.: An AEROdynamic Best Estimate Trajectory File (AEROBET) for NASA Langley Research Center Shuttle Investigations. AMA Report 82-9, Analytical Mechanics Associates, Inc., March 1982.

10. Flanagan, P. F.: Final Report/GTFILE Generation - Definition and Development. AMA Report 81-20, Analytical Mechanics Associates, Inc., July 1981.

11. Maine, Richard E.; and Iliff, Kenneth W.: User's Manual for MMLE3, a General FORTRAN Program for Maximum Likelihood Parameter Estimation. NASA TP-1563, 1980.

12. Murphy, Patrick C.: An Algorithm for Maximum Likelihood Estimation Using an Efficient Method for Approximating Sensitivities. NASA TP-2311, June 1984.

13. Price, Joseph M.: Atmospheric Definition for Shuttle Investigations. Journal of Spacecraft and Rockets, vol. 20, pp. 133-140, March-April 1983.

14. Compton, Harold R.; Findlay, John T.; Kelly, George M.; and Heck, Michael L.: Shuttle (STS-1) Entry Trajectory Reconstruction. AIAA Paper No. 81-2459, 1981.

15. Maine, Richard E.; and Iliff, Kenneth W.: Selected Stability and Control Derivatives from the First Three Space Shuttle Entries. AIAA Paper No. 82-1318, 1982.

Table I Comparison of Trim Curve and Parameter Ratios

Mach Number	Aileron Trim/ Beta Trim	Flight $\frac{C_{\ell_\beta}}{C_{\ell_{\delta a}}}$	Predicted $\frac{C_{\ell_\beta}}{C_{\ell_{\delta a}}}$
1	.93	.91	.93
3	2.32	2.04	1.96
4	2.5	3.23	2.0
6	1.82	1.67	1.43
22	1.41	1.39	1.32

Table II Parameters Extracted from Different Discovery Inputs at Mach = 8 for Inputs of Figure 5

Parameter	Input 1	Input 2
C_{Z_0}	-1.03	-.96
C_{Z_α}	-4.58	-.78
C_{m_α}	-.11	-.15
$C_{m_{\delta e}}$	-.16	-.13

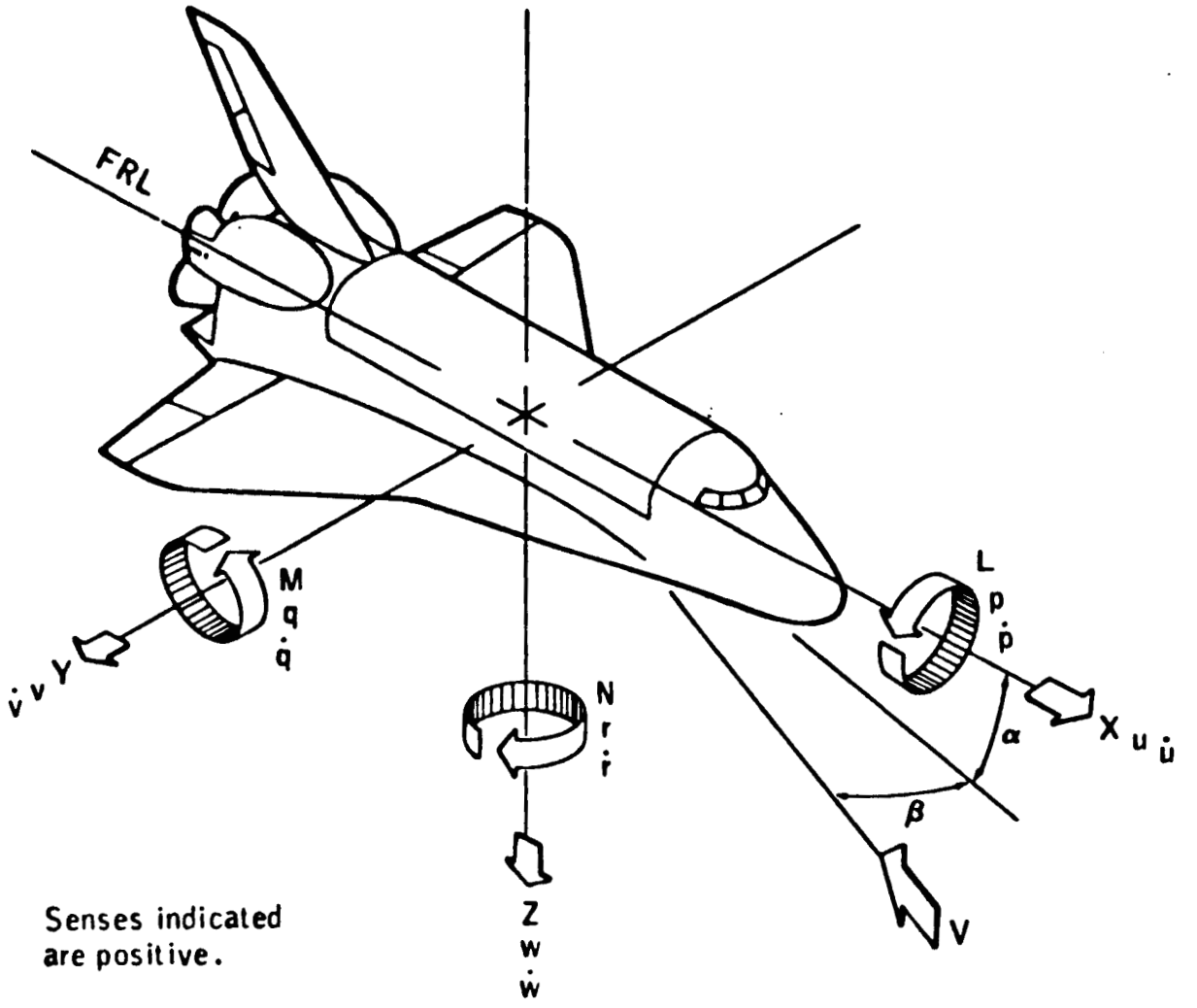

Figure 1.- Schematic of Shuttle vehicle showing body axes and positive senses of accelerations, rates, velocities, moments and angles.

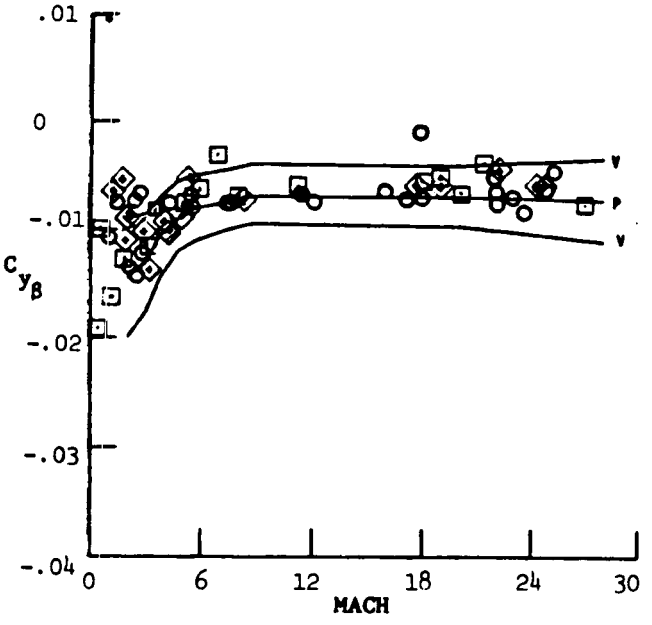

(a) Sideforce

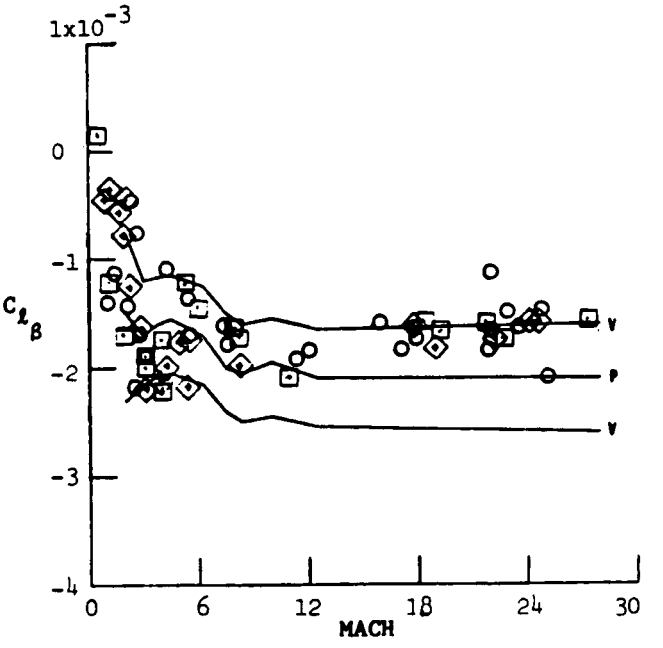

(b) Rolling Moment

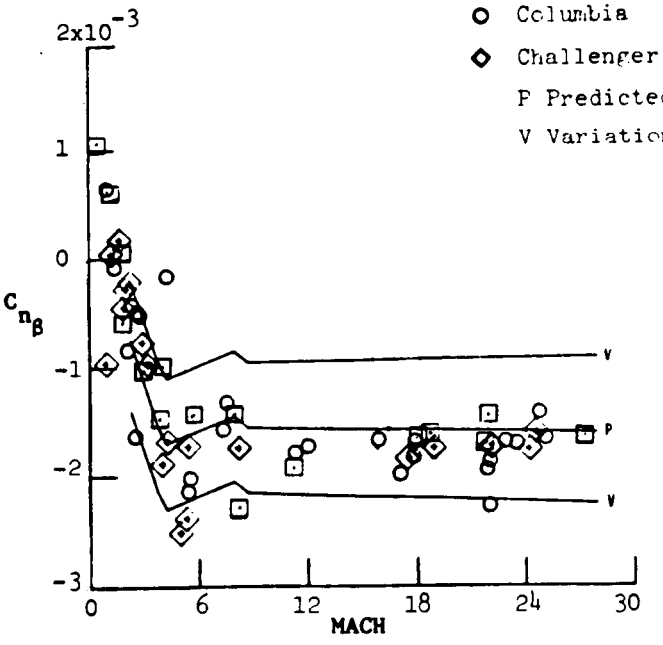

(c) Yawing Moment

□ Discovery
○ Columbia
◇ Challenger
P Predicted
V Variations

Figure 2.- Sideslip derivatives versus Mach Number (derivatives per degree).

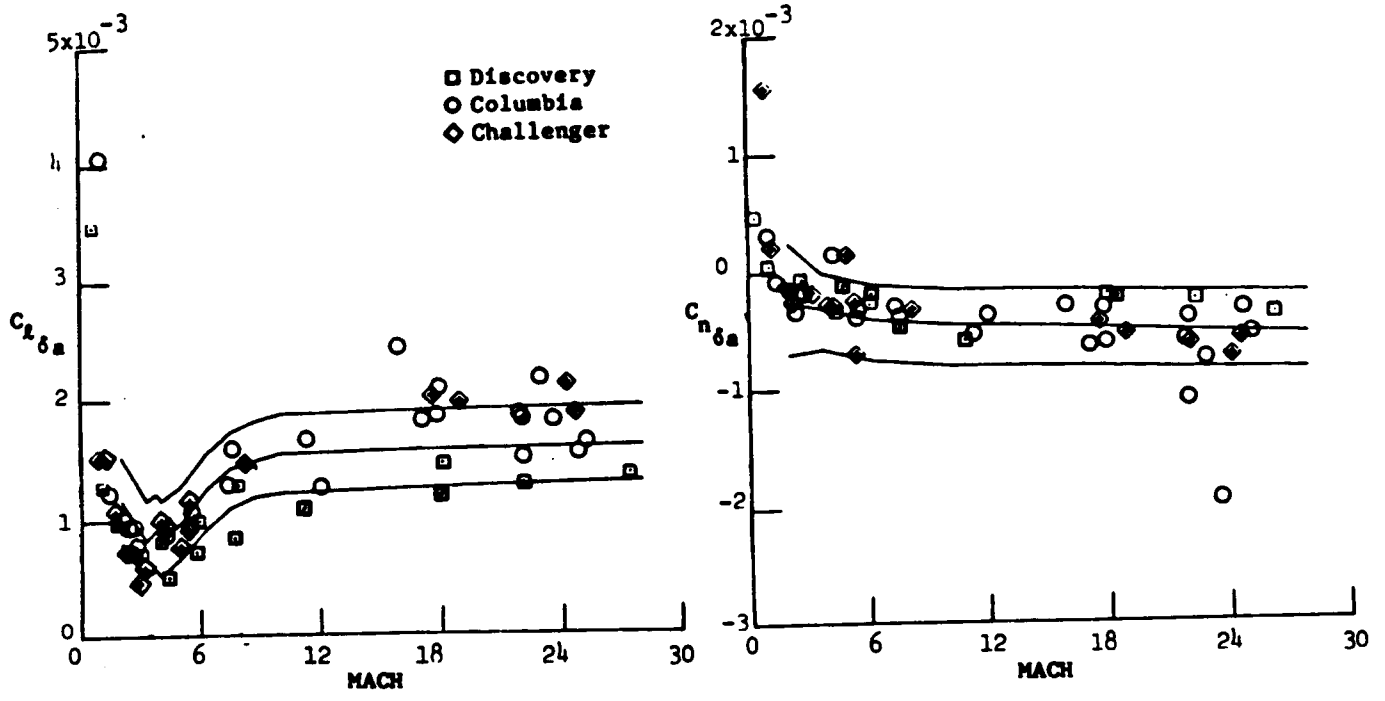

(a) Rolling Moment

(b) Yawing Moment

Figure 3. - Aileron effectiveness.

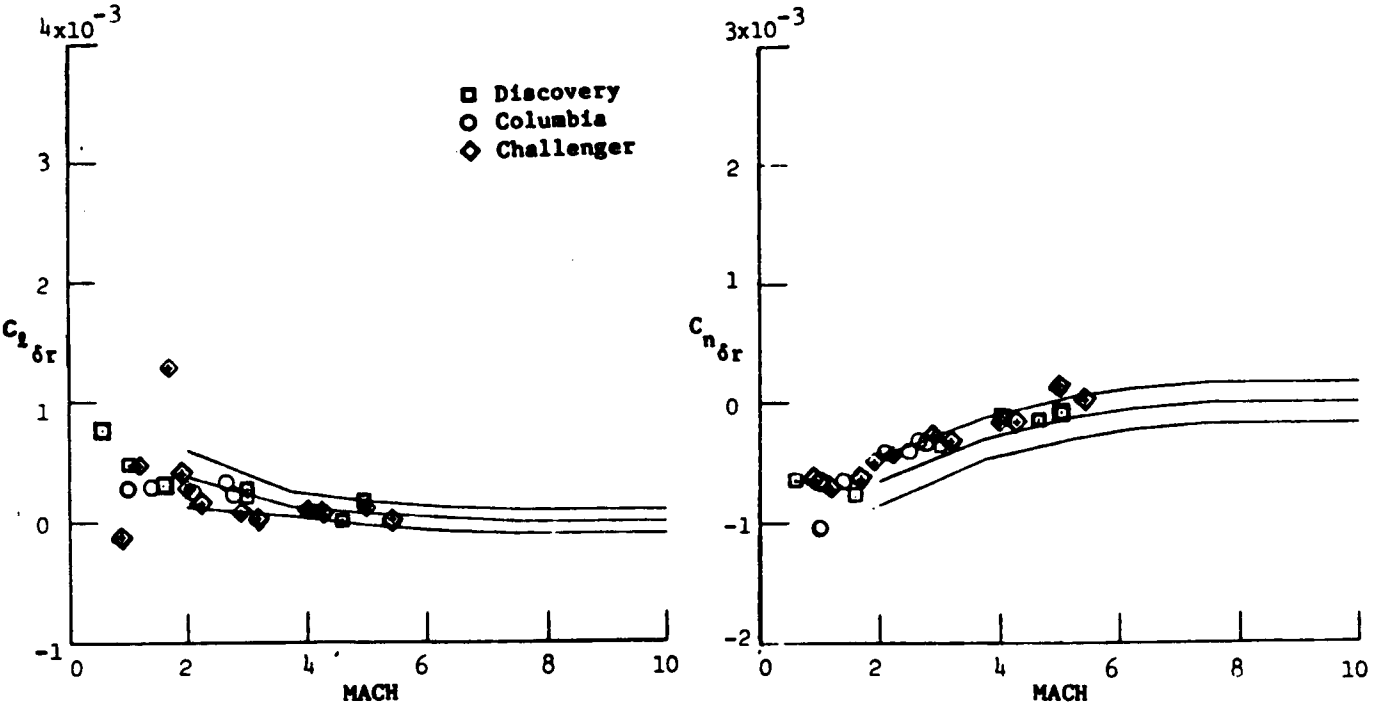

(a) Rolling Moment

(b) Yawing Moment

Figure 4. - Rudder effectiveness.

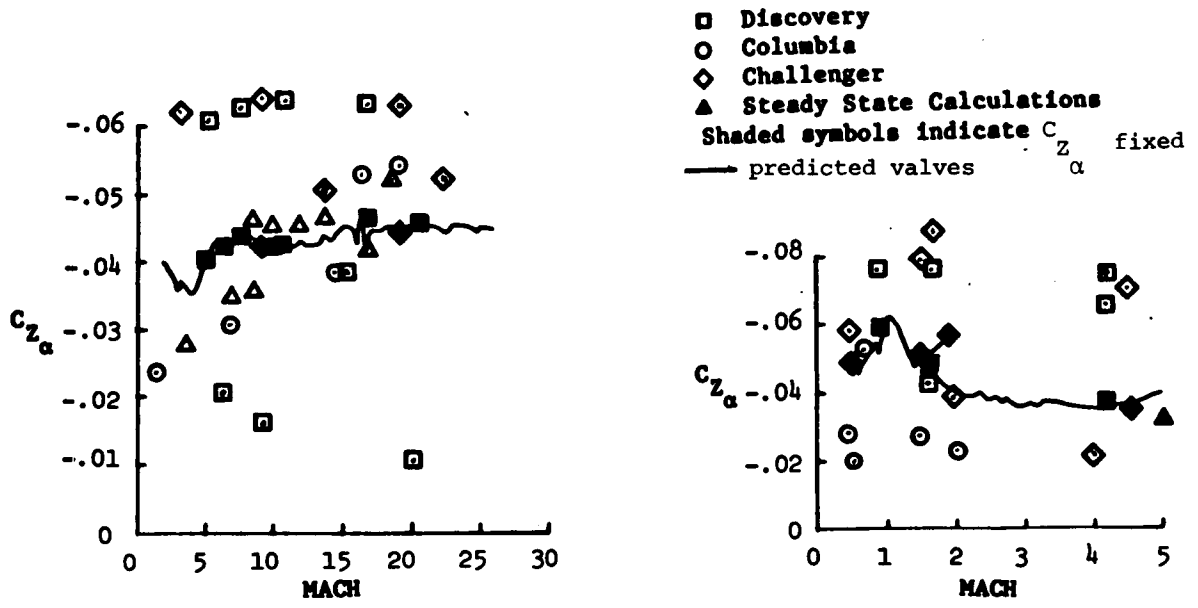

(a) Change in normal force with alpha

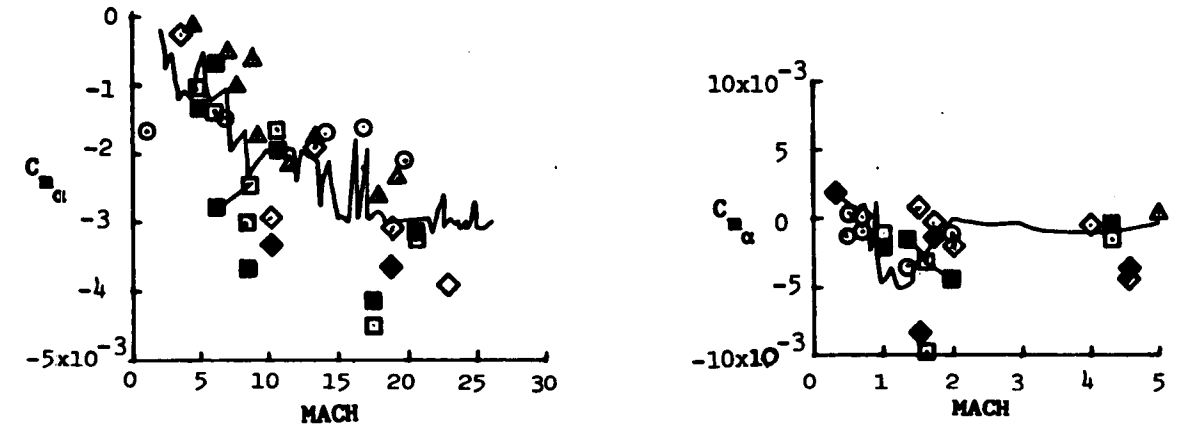

(b) Static stability

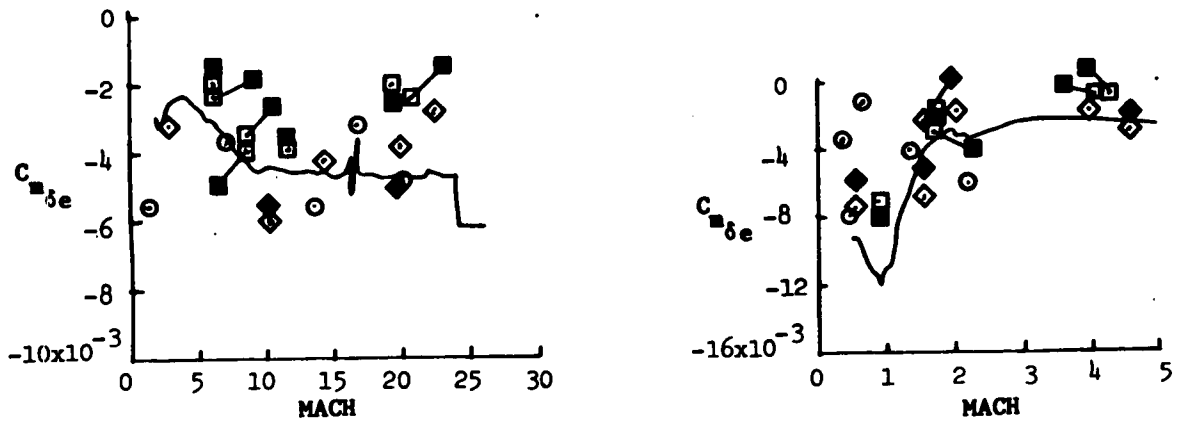

(c) Elevon effectiveness

Figure 5.— Dominant longitudinal derivatives affecting the short period motion of the Shuttle versus Mach number (derivatives per degree).

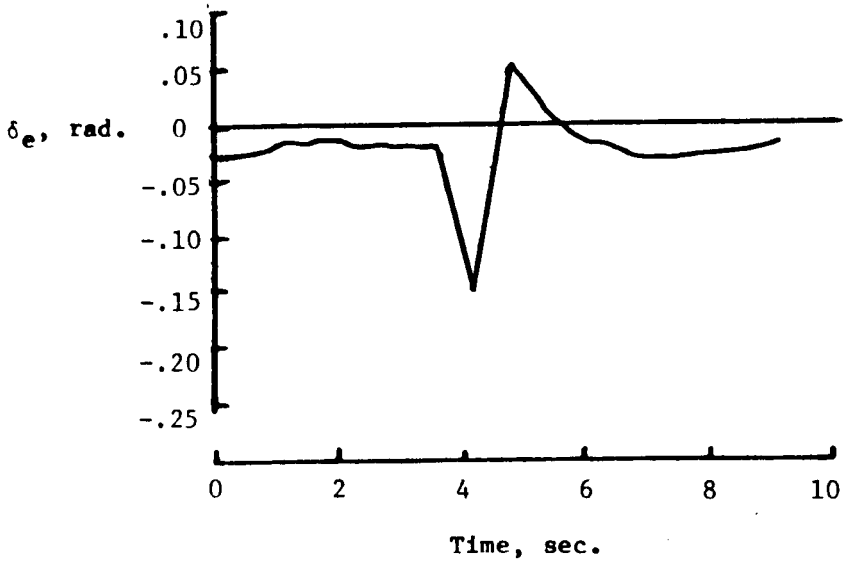

(a) Input 1 (First Discovery Flight)

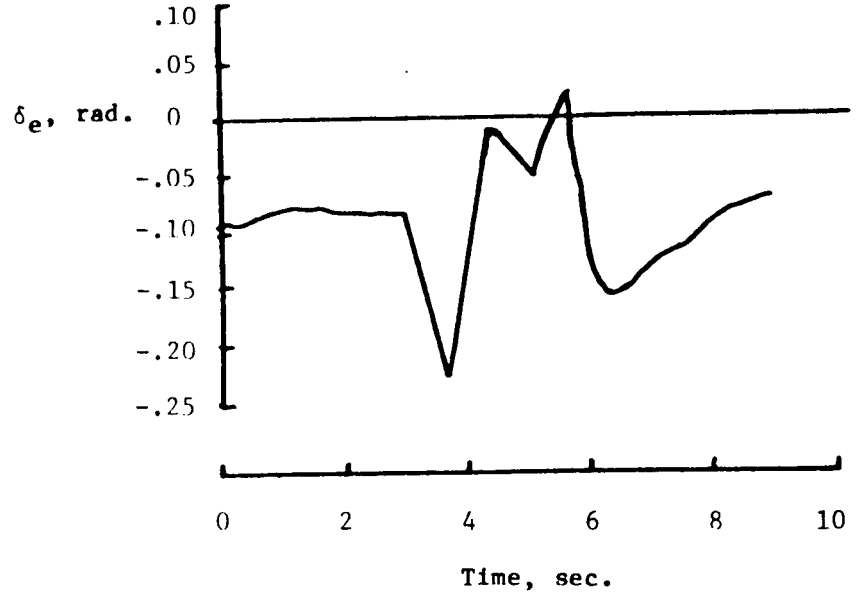

(b) Input 2 (Second Discovery Flight)

Figure 6.— Elevon control inputs used for Discovery parameter identification Mach > 5.

NASA
National Aeronautics and Space Administration

Report Documentation Page

1. Report No.	2. Government Accession No.	3. Recipient's Catalog No.
NASA TM-100555		

4. Title and Subtitle

Lateral and Longitudinal Stability and Control Parameters for the Space Shuttle Discovery as Determined from Flight Test Data

5. Report Date

February 1988

6. Performing Organization Code

7. Author(s)

William T. Suit and James R. Schiess

8. Performing Organization Report No.

10. Work Unit No.

506-46-21-01

9. Performing Organization Name and Address

NASA Langley Research Center
Hampton, VA 23665-5225

11. Contract or Grant No.

13. Type of Report and Period Covered

Technical Memorandum

12. Sponsoring Agency Name and Address

National Aeronautics and Space Administration
Washington, DC 20546-0001

14. Sponsoring Agency Code

15. Supplementary Notes

16. Abstract

The Discovery vehicle was found to have longitudinal and lateral aerodynamic characteristics similar to those of the Columbia and Challenger vehicles. The values of the lateral and longitudinal parameters are compared with the pre-flight data book. The lateral parameters showed the same trends as the data book. With the exception of C_{ℓ_β} for Mach numbers greater than 15, $C_{n_{\delta r}}$ for Mach numbers greater than 2 and for mach numbers less than 1.5, where the variation boundaries were not well defined, ninety percent of the extracted values of the lateral parameters fell within the predicted variations.

The longitudinal parameters showed more scatter, but scattered about the pre-flight predictions. With the exception of the Mach 1.5 to .5 region of the flight envelope, the preflight predictions seem a reasonable representation of the Shuttle aerodynamics. The models determined accounted for ninety percent of the actual flight time histories.

17. Key Words (Suggested by Author(s))	18. Distribution Statement
Parameter Estimation Stability and Control Parameters Maximum Likelihood	Unclassified-Unlimited Subject Category 08

19. Security Classif. (of this report)	20. Security Classif. (of this page)	21. No. of pages	22. Price
Unclassified	Unclassified	23	A02

NASA FORM 1626 OCT 86 FOR SALE BY THE NATIONAL TECHNICAL INFORMATION SERVICE, SPRINGFIELD, VA 22161-2171